JOURNAL OF GEOPHYSICAL RESEARCH, VOL. 89, NO. C4, PAGES 6494–6504, JULY 20, 1984

The Seasonal Variation of the Mixed Layer and the Pycnocline Under Polar Sea Ice

P. LEMKE

Max-Planck-Institut für Meteorologie

T. O. MANLEY

Lamont-Doherty Geological Observatory of Columbia University

A model of the seasonal variation of the mixed layer and the pycnocline under polar sea ice is compared with observations during the Arctic Ice Dynamics Joint Experiment (AIDJEX) 1975–1976. The model is of the Kraus-Turner type, extended to include mixed layer and pycnocline. The forcing mechanisms are the mechanical mixing due to ice keel stirring and the surface buoyancy flux due to melting and freezing of sea ice. The model is designed to be used for climate studies in conjunction with atmospheric and oceanic general circulation models and with sea ice models.

1. INTRODUCTION

Models for the oceanic mixed layer are of special importance in climate-related problems, since the mixed layer represents the link between the atmosphere and the interior ocean. Recently, oceanic general circulation models (GCM's) have been improved to include a variable depth mixed layer [*Kim and Gates*, 1980; *Adamec et al.*, 1981; *Pollard et al.*, 1983] in order to better represent the upper layers of the ocean and the interaction with the atmosphere. These upper-ocean models generally consist of a one-dimensional entrainment and retreat model and a three-dimensional advection scheme, which are embedded in multilevel primitive equation GCM's.

In this paper we will present an alternative model, especially suited for polar oceans, which later will replace the upper levels of an oceanic GCM and will be coupled to a sea ice model similar to that of *Pollard et al.* [1983]. Since mixed layer models generally contain a number of adjustable parameters, the main purpose of this paper is to objectively derive the optimal model structure and the values of the model parameters from a least squares comparison to observations rather than by intuitively tuning the model parameters. The main emphasis will be on the one-dimensional model for the vertical exchange processes in the mixed layer and the pycnocline, since the existing data is insufficient to be used in a three-dimensional model fit. However, we will briefly describe how advection enters into the model. The time scales discussed are seasonal rather than daily.

There are a variety of models that describe the time evolution of the mixed layer properties in the open ocean, where wind mixing and seasonal varying heating and cooling are the dominant forcing mechanisms that form the mixed layer. For a review, see *Niiler and Kraus* [1977].

Despite the heavy ice cover, a well-developed mixed layer is obsered in the Arctic Ocean [*McPhee*, 1978; *Morison and Smith*, 1981]. In this case the dominant forcing mechanisms are the buoyancy flux associated with the ice freezing (brine convection) and mechanical mixing due to keel stirring induced by the ice motion. Observations during the Arctic Ice Dynamics Joint Experiment (AIDJEX) 1975–1976, show that during most parts of the year the base of the mixed layer is sharply defined; its depth varies from 60 m in late winter to 20 m in summer. The salinity varies from 30.5‰ to 29.8‰, respectively. The data indicate that the mixed layer temperature exhibits almost no seasonal cycle and is near the freezing point down to well below the winter mixed layer [*McPhee*, 1978], i.e., the net heat flux is mainly used to melt and freeze ice. The density is predominantly controlled by salinity.

In this paper a quantitative description of the observed salinity profiles during AIDJEX is achieved from a one-dimensional model for the mixed layer and the pycnocline, which is an extension of a polar mixed layer model developed by the senior author during the Woods Hole Summer Study Program in Polar Oceanography [*Lemke*, 1979]. The model is vertically parameterized and can be integrated sufficiently fast in order to be used for climate studies in conjunction with atmospheric and oceanic GCM's and sea ice models.

According to the observed vertical density profiles, which are fairly homogeneous in the mixed layer and show a continuous increase in the pycnocline, the vertical density structure of our two-layer model is described by four parameters (see Figure 1): the mixed layer depth h, a constant density ρ within the mixed layer, a scale depth d that describes the thickness of the pycnocline, and the asymptotic density ρ_∞ for $z \to -\infty$. The density profile is given by

$$\begin{aligned} \rho(z) &= \rho && 0 > z > -h \\ \rho(z) &= \rho_\infty + (\rho - \rho_\infty) \exp\,[(z + h)/d] && -h > z > -h_b \end{aligned} \tag{1}$$

The lower level of our model h_b is set at 150 m. The data show that generally, $h_b - h \gg d$, so that $\rho_b = \rho(-h_b) \approx \rho_\infty$. The density ρ can be interpreted in terms of temperature and salinity, but since the density in the Arctic Ocean is dominated by the latter, we will restrict our discussion in this paper to salinity S, mixed layer depth h, and e-folding depth d of the pycnocline. The evolution of these three variables is determined from prognostic equations, and ρ_b is given as a boundary condition. A similar model has been applied to temperature profiles observed at North Atlantic weathership stations by *Maier-Reimer et al.* [1982].

Paper number 4C0298.
0148-0227/84/004C-0298$05.00

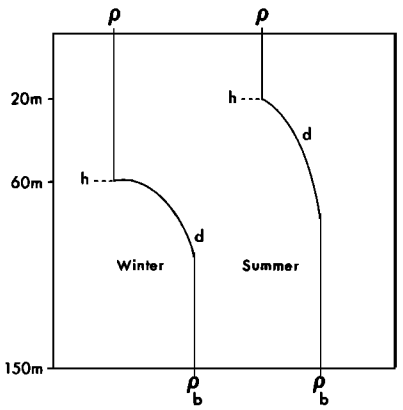

Fig. 1. Vertical structure of the mixed layer–pycnocline model.

2. DATA

The main AIDJEX program (1975–1976) was designed to obtain data on the meso- and macroscale interactions of the wind-ice-water system in order to provide information that may lead to improvements in the modeling of an ice-covered ocean [*Pritchard*, 1980]. The major part of the experiment consisted of meteorological and oceanographic programs on four manned drifting ice camps in the Beaufort Sea. The manned camps were initially established in an array with three satellite camps forming a triangle centered around a larger main camp. Spacing between the satellite camps was nominally 100 km and the duration of the experiment was one year, April 1975 to April 1976. A map of the AIDJEX operational area is shown in Figure 2, including the beginning and ending positions of the manned camps superimposed on the dynamic topography of the Beaufort Sea.

The original main camp was Big Bear, and the satellite camps were Snowbird, Blue Fox, and Caribou. During the course of the experiment, Big Bear was evacuated due to severe ice breakup during late September of 1975. Caribou then became the main camp for the remaining duration of the experiment. Satellite positioning of the manned camps [*Thorndike and Manley*, 1980*a*, *b*] was used to provide accurate movement of the local ice field (position, velocity, and acceleration) to determine its response to the driving forces of wind and water.

The oceanographic program was designed to observe the temperature, salinity and current structure of the upper ocean (above 800 m), thereby providing estimates of the momentum and stress balance between the ice and water [*Hunkins*, 1974,

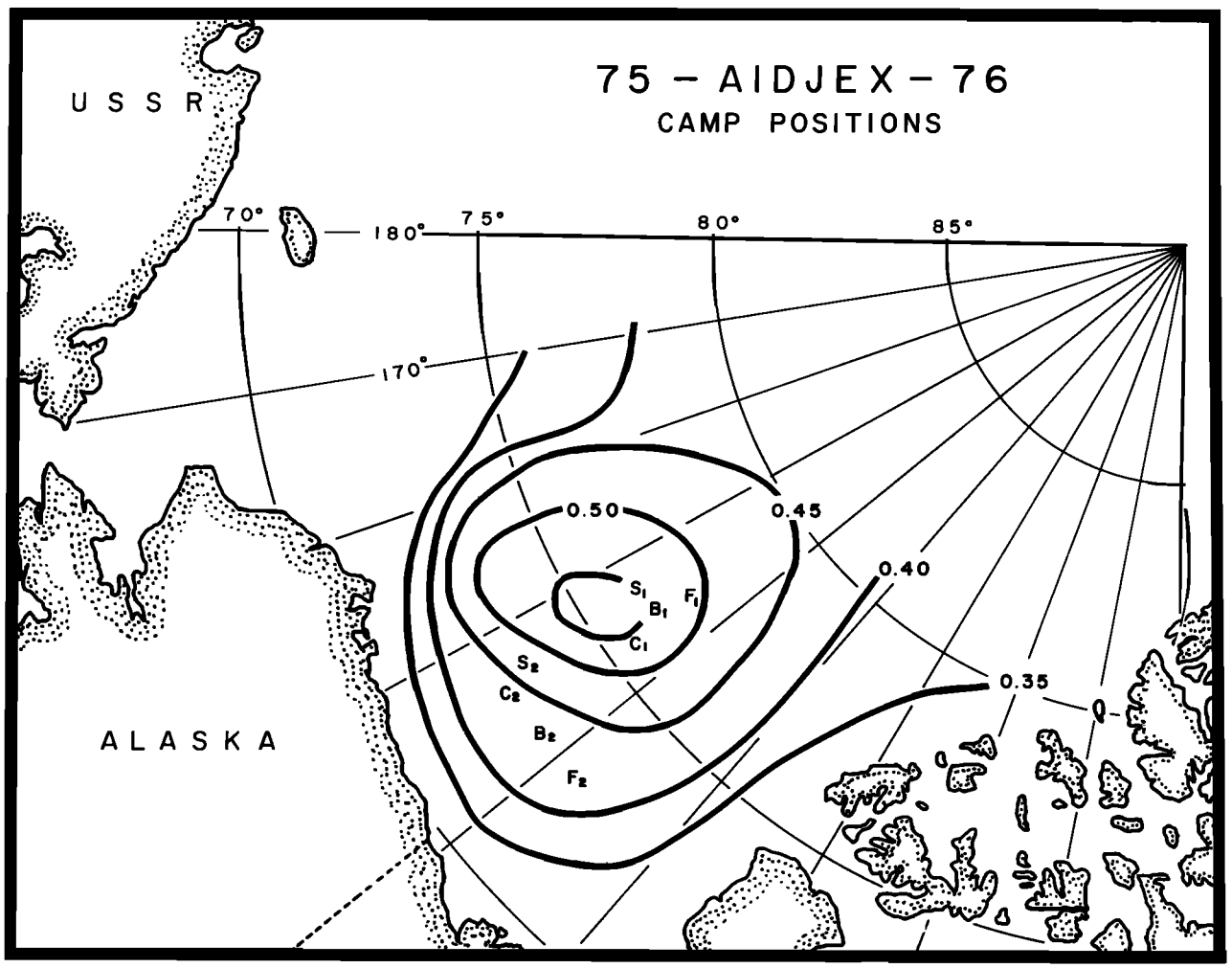

Fig. 2. Beginning and ending positions of the AIDJEX 1975–1976 manned camps superimposed on the mean dynamic topography [*Newton*, 1973] of the Beaufort Sea. Abbreviations are C (Caribou), F (Blue Fox), S (Snowbird), and B (Big Bear). Subscripts 1 and 2 indicate the beginning and ending positions of the camps, respectively.

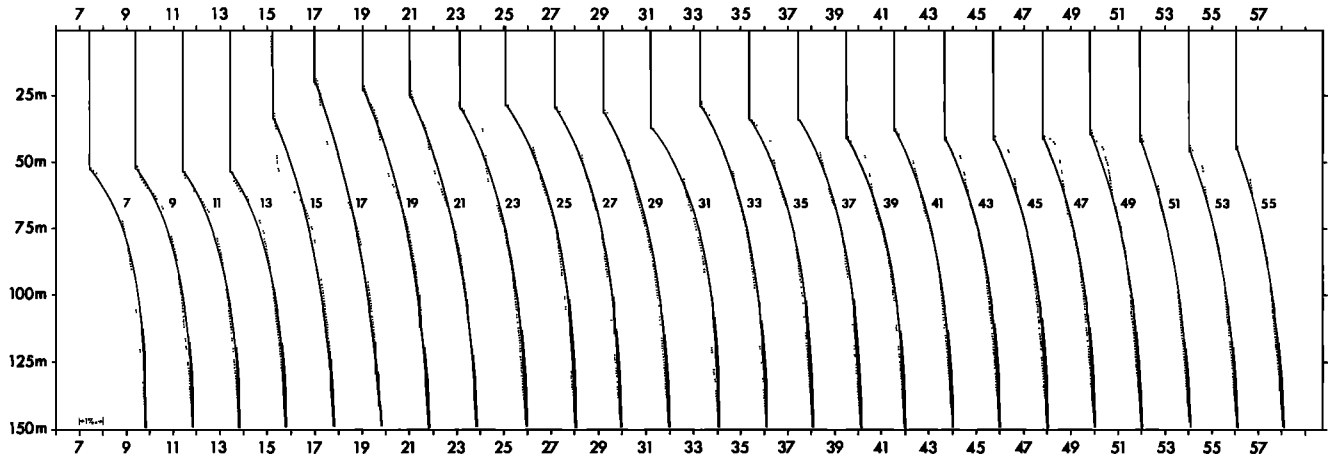

Fig. 3. Observed (dotted lines) and optimally fitted model salinity profiles (solid lines) for camp Caribou covering AIDJEX weeks 7 to 55. The upper and lower tic marks refer to 30.0‰ and have a spacing of 1‰.

1975; *McPhee and Smith*, 1976]. Salinity and temperature observations were taken at each of the manned camps, usually once daily to a depth of 750 meters with Plessey model 9040 STD (salinity, temperature, and depth) and CTD (conductivity, temperature, and depth) systems. At the main camp, two casts were taken daily as well as a weekly deep cast to 3000 meters. Reversing thermometers and salinity samples were taken at several depths in the water column at each of the camps in order to provide accurate sensor calibration. Salinity samples taken at the satellite camps were flown to the main camp, where they were analyzed. During the yearlong experiment a total of 1287 vertical STD profiles were collected for the AIDJEX oceanographic data base. More information on this data base is given by *Bauer et al.* [1980*a*, *b*, *c*, *d*].

For this study, only weekly averages of the salinity profiles down to 150 m were used. A large number of mesoscale eddies were observed throughout the AIDJEX 1975–1976 Experiment [*Manley*, 1981] within the depth range of 50 to 300 m and as a result would potentially be a source of salinity contamination during the weekly averaging process. The eddies themselves had an estimated average diameter of 20 km and thickness of 200 meters. A comparison was made between the weekly salinity averages with and without those STD stations associated with the eddies. As it turned out, the differences were slight, since stations associated with eddies within any given week were few when compared to the total number of stations, and the salinity deviations associated with the eddy field were less than a few tenths of a part per thousand from the local norm. As a result, all STD casts were used in the averaging process.

In order to verify the model briefly outlined in the introduction, profiles of the form (1) were fitted to the observed AIDJEX salinity data. The mixed layer depth h was given as the smallest depth at which the salinity increases by more than 0.1‰. The mixed layer salinity S was determined as the vertical average from 0 to h. S_b was taken as the observed salinity at 150 m, and d was derived from a least squares fit to observed salinity data between h and h_b. Examples of the optimal profile fit (solid lines) are shown in Figures 3 and 4 for Caribou and Snowbird data (dotted lines), respectively. The two-layer fit represents many profiles comparatively well, especially for Snowbird, where the remnant of the winter pycnocline is visible only during the short summer and is destroyed by turbulent processes later in the year. During the

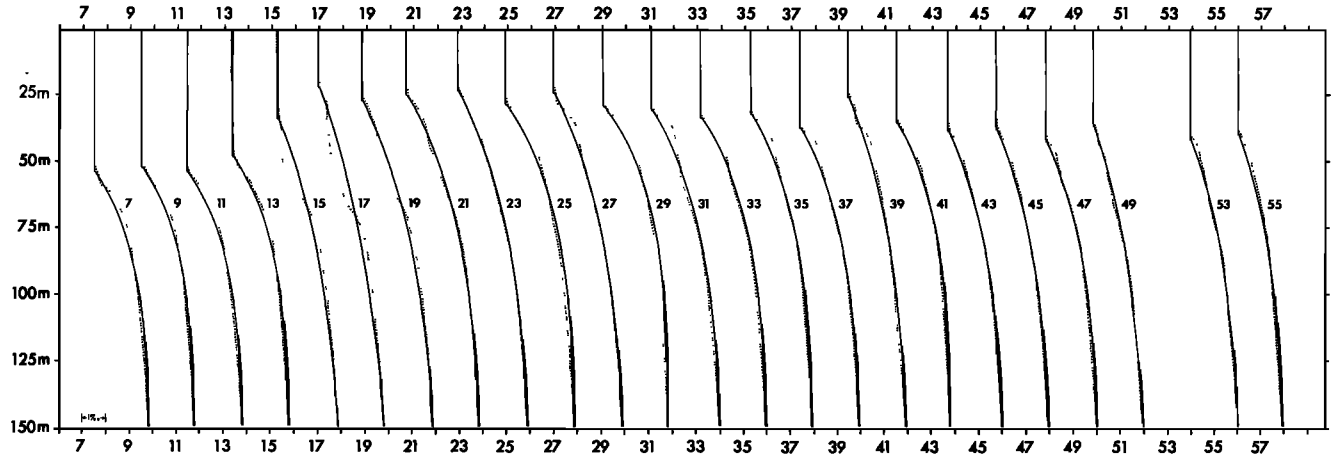

Fig. 4. Observed (dotted lines) and optimally fitted model salinity profiles (solid lines) for camp Snowbird covering AIDJEX weeks 7 to 55. The upper and lower tic marks refer to 30.0‰ and have a spacing of 1‰.

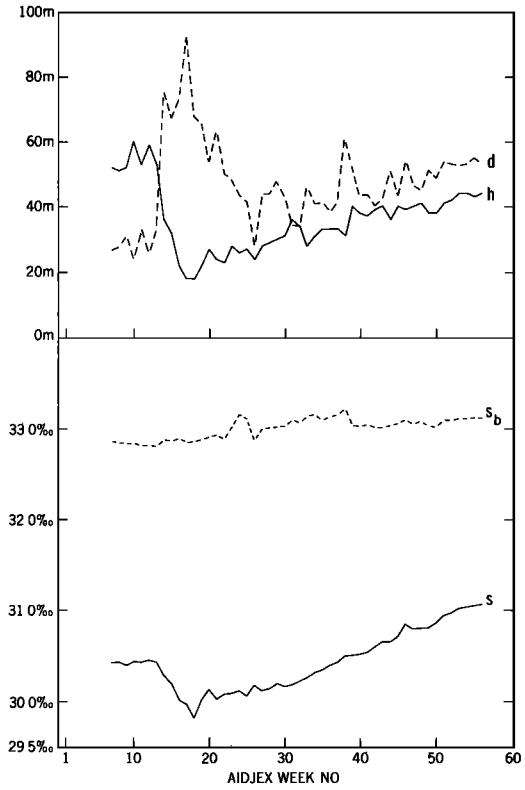

Fig. 5. Least squares fitted salinity profile variables during AIDJEX for camp Caribou: mixed layer salinity S, mixed layer depth h, salinity at 150 m depth S_b, and e-folding depth of the pycnocline d.

short retreat of the mixed layer in summer the stratification shows two exponential layers below the mixed layer rather than one, but this will not be pursued further in this paper. Compared to the treatment of the upper ocean in oceanic GCM's (usually three layers of fixed depth in the upper 150 m, with depth independent density within each layer), the present model, with variable mixed layer depth, salinity, and pycnocline thickness as described in the next section, should provide an improvement in the modeling of the vertical density structure.

The time series of the fitted parameters for the model profile for Caribou are shown in Figure 5. The corresponding time series for Snowbird and Blue Fox show similar characteristics. It is seen that the seasonal cycle is limited to the mixed layer depth h, the mixed layer salinity S, and the e-folding depth d of the pycnocline. The salinity at 150 m depth, S_b, shows no seasonal variation.

It is also seen that the data are not cyclostationary. The observed annual increase in S, S_b, and d and decrease in h may have been introduced by noncyclostationary surface fluxes and/or advection in the ocean, but we believe that this trend is largely due to the drift of the ice floes on which the AIDJEX camps were located (see Figure 2), thereby collecting information on tracks of several hundred kilometers length. Without additional data on the time histories (seasonal cycles) of surface fluxes, ocean currents, and horizontal gradients of the salinity field, these three effects cannot be distinguished from each other. The drift of the AIDJEX camp presumably represents the largest source of data contamination because the ice velocity was generally larger than the ocean currents.

3. Model

The mixed layer model presented in this section is divided into two parts. A one-dimensional entrainment and retreat model of the Kraus-Turner type, extended to include the pycnocline, describes the vertical mixing processes. Here the evolution of the three prognostic variables, S, h, and d, is determined through the conservation of salt in the two-layer water column, potential energy considerations, and a closure hypothesis that correlates changes of d with changes of the mixed layer depth h and salinity S. The change of the profile parameters S, h, and d due to advection is addressed in a three-dimensional model by using the continuity equation and the conservation of salt in both layers separately. There is no exchange between mixed layer and pycnocline in this part of the model: that is taken care of by the one-dimensional entrainment model.

For the open ocean, where the density is dominated by the temperature, a similar model may be applied for temperature T, mixed layer depth h, and thermocline thickness d, the conservation of salt being then replaced by conservation of heat [*Maier-Reimer et al.*, 1982]. Generally, both the temperature and salinity equations have to be used in global oceanic circulation models.

In our one-dimensional model the salt balance states that the change of salt content of the two-layer ocean column is balanced by the effective salt fluxes at the surface, Q_S, which are due to the melting and freezing of sea ice. With the assumption $h_b - h \gg d$, the salt content

$$H = \int_{-h_b}^{0} S(z)\, dz$$

is given by

$$H = (S - S_b)(h + d) + S_b h_b \tag{2}$$

Taking the derivative with respect to time yields

$$\dot{H} = \dot{S}(h + d) + (\dot{h} + \dot{d})(S - S_b) \tag{3}$$

with

$$\dot{H} = Q_S \tag{4}$$

The term accounting for changes in S_b is omitted in the entrainment part of the model, since variations in S_b are believed to be caused by advection rather than by vertical mixing processes which originate at the sea surface. S_b is treated as a given boundary condition, which will be determined by the coupling to the deep ocean part of the oceanic GCM.

The data (Figure 5) indicate that during deepening of the mixed layer the steepness of the profile in the seasonal pycnocline is increased, whereas it is decreased during the retreat of the mixed layer, i.e., the correlation between d and h is negative. Allowing also for changes in d with respect to the mixed layer salinity, our assumption for the second prognostic equation is

$$\dot{d} = -\alpha_1 \dot{h} + \alpha_2 \dot{S} \tag{5}$$

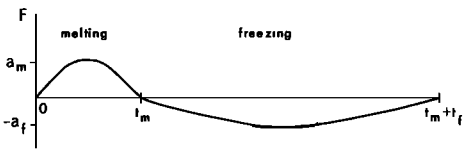

Fig. 6. Annual cycle of model surface salt flux.

This is an empirical relationship which will be tested by a least squares fit to observations (section 5), which will also provide the optimal values for the constants α_1 and α_2. Inserting (5) into (3) we find for the mixed layer salinity

$$\dot{S} = \frac{Q_s + (S_b - S)(1 - \alpha_1)\dot{h}}{h + d - \alpha_2(S_b - S)} \tag{6}$$

The first term in the numerator on the right-hand side of (6) describes salinity changes in the mixed layer due to surface fluxes, and the second term denotes the effect of the entrainment flux, i.e., the exchange of salt between the mixed layer and the pycnocline. It is clear from (6) that for meaningful results α_1 is limited to the range $0 \leq \alpha_1 \leq 1$ and $\alpha_2 < (h + d)/(S_b - S)$. It will be shown in section 5 that this is consistent with observations. It is also clear that as long as $\alpha_1 \neq 1$, there is no need to introduce a density discontinuity at the mixed layer base to generate an entrainment buoyancy flux, as is usually done in Kraus-Turner type models [see *Niiler and Kraus*, 1977]. The data actually do not show pronounced discontinuities but more or less sharp continuous profiles below the mixed layer base.

Although not originally designed as a microprofiler, the Plessey did record step structure of the order of 2 meters in thickess and greater. This was primarily evident on the high-resolution digital data and was more commonly found in the depth range of 100 to 500 meters. The thickness of the pycnocline is generally substantially larger than the resolution of the Plessey.

As usual in Kraus-Turner type models the closure for the mixed layer depth is taken from potential energy considerations. The first closure we investigated was the assumption that the surface kinetic energy input due to wind or ice keel stirring balances the potential energy change in the two-layer column (mixed layer plus pycnocline). It turned out that in the Arctic Ocean, where the stability is relatively large, the seasonal variations of the pycnocline thickness, which are largely due to vertical mixing process, represent the dominant term in the potential energy balance.

The assumption of a negative correlation between variations in d and h (equation (5)) created a singularity in the differential equations for a particular value of the constant $\alpha_1 = \alpha_{crit}$. The critical value α_{crit} is a function of the profile parameters and of α_2 and is generally of the order of $\alpha_{crit} < 0.3$. Physical meaningful results are only obtained for $\alpha_1 < \alpha_{crit}$. This model provided a relatively good description for the annual variation of mixed layer salinity and depth and a somewhat poorer modeling of the pycnocline, but the main disadvantage was that the parameters α_1 and α_2 had to be chosen to be near the singularity.

Therefore in the following we will restrict the potential energy considerations to the mixed layer alone, the assumption being, as in Kraus-Turner type models, that wind or ice keel stirring provides the only energy $\tilde{Q}_w$ needed to balance the increase of the potential energy due to the surface and entrainment salt fluxes, Q_s and Q_e, respectively. We will assume that there is always enough turbulence in the pycnocline layer to provide energy required for changes of the pycnocline shape (equation (5)).

Other turbulent kinetic energy sources for the mixed layer besides surface stress and convection are neglected. The vertical shear in the Arctic Ocean is relatively small, and the importance of internal waves on the Arctic mixed layer has not been demonstrated yet, although it has recently been shown in laboratory experiments that up to 30% of the apparent drag on an ice keel may be due to the interactions between the keel and interfacial internal waves on the pycnocline [*Muench et al.*, 1983]. Whether or not the internal waves would lead to local mixing or propagate from the region taking energy with them remains, for now, an open question.

The potential energy balance for the entrainment phase of the annual cycle then reads

$$\tilde{Q}_w - \varepsilon = \frac{h}{2} g\beta(Q_e - Q_s) \tag{7}$$

where g is the gravitational acceleration and β is the expansion coefficient of the density with respect to salinity; ε denotes a dissipation term which will be explained later. From (6) we find the entrainment salt flux Q_e through multiplication of the entrainment-induced salinity change with the mixed layer depth:

$$Q_e = h \frac{(S_b - S)(1 - \alpha_1)\dot{h}}{h + d - \alpha_2(S_b - S)} \tag{8}$$

inserting (8) into (7) and rearranging terms leads to

$$g\beta \frac{h^2}{2} \frac{(S_b - S)(1 - \alpha_1)\dot{h}}{h + d - \alpha_2(S_b - S)} = \tilde{Q}_w + g\beta \frac{h}{2} Q_s - \varepsilon \tag{9}$$

The left-hand side of (9) represents the work per unit time necessary to mix the dense entrained water through the mixed layer. $\tilde{Q}_w$ is the rate of working by the wind or ice keel stirring, and the second term on the right-hand side denotes the rate of potential energy change produced by fluxes across the sea surface. For $d = \alpha_1 = \alpha_2 = 0$, i.e., when there is a step at the mixed layer base, (5), (6), and (9) reduce to the well-known Kraus-Turner type model.

The dissipation term ε in (9) is parameterized according to *Niiler and Kraus* [1977] in terms of the active turbulence generating processes: windstirring $\tilde{Q}_w$ and convection (second term on the right-hand side of (9), in winter only when Q_s is positive). Equation (9) then reads

$$\dot{h} = \frac{2Q_w D_w + hQ_s D_s}{h^2(S_b - S)(1 - \alpha_1)} [h + d - \alpha_2(S_b - S)] \tag{10}$$

where $Q_w = \tilde{Q}_w/g\beta$.

D_w and D_s describe the depth-dependent dissipation of mechanical and convective energy input at the surface. This depth dependence is assumed to be exponential [*Niiler and Kraus*, 1977]:

$$D_w = \exp(-h/h_w) \tag{11}$$

$$\begin{aligned} D_s &= 0 && Q_s < 0 \\ D_s &= \exp(-h/h_c) && Q_s > 0 \end{aligned} \tag{12}$$

where h_w and h_c are the scale depths of dissipation for surface mechanical energy input and convection, respectively.

Introducing the dissipation also for convection takes care of one problem that occurs in one-dimensional mixed layer modeling: the net annual kinetic energy input due to the surface stress leads to a continuous deepening of the mixed layer. In order to obtain a stable seasonal cycle, this excess energy has to be destroyed by mechanisms like a "background dissipation" [*Niiler*, 1977], by a small upwelling, or by dissipating convective energy. All three methods reduce the potential energy of the system. There is no general consensus on which mechanism should be preferred. Introduction of an upwelling

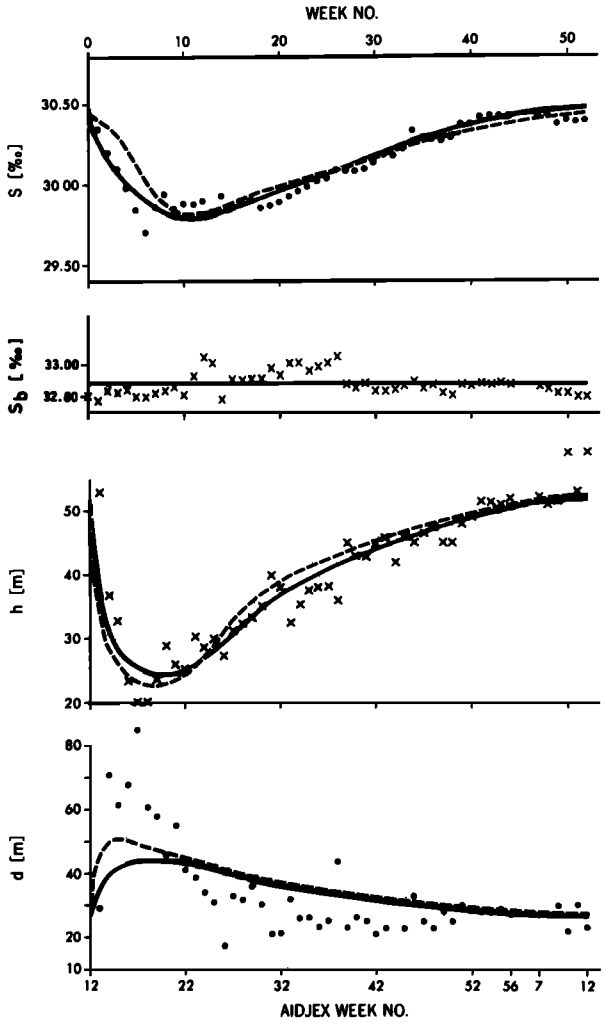

Fig. 7. Observed detrended salinity profile variables for camp Caribou (dots, crosses) and optimally simulated equilibrium annual cycles for model I*a* (solid lines) and model I*b* (dashed lines).

also requires a net surface buoyancy source in order to balance the net entrainment of denser water into the mixed layer and thereby obtain a cyclostationary response. Both the dissipation mechanisms do not require this extra source.

Equations (5), (6), and (10) apply for the entrainment phase of the seasonal cycle ($\dot{h} > 0$). If the right-hand side of (10) becomes negative, the stress induced energy at the sea surface is insufficient to overcome the stabilizing effect of the surface buoyancy flux. This phase of no entrainment occurs during the period of increased heating (melting). The mixed layer then retreats to an equilibrium depth (the Monin-Obukhov length) $\hat{h}$ which is, as usual, diagnostically determined from (10) with $\dot{h} = 0$ or

$$2Q_w D_w + \hat{h} Q_s D_s = 0 \tag{13}$$

where D_w and D_s are given by (11) and (12) with h replaced by $\hat{h}$. The evolution of the mixed layer salinity S and the pycnocline thickness d follows from (5) and (6), where the entrainment rate $\dot{h}$ is now replaced by the diagnostic retreat $\Delta h/\Delta t$ of the mixed layer. This method (henceforth called model II*a*) was found to provide the smallest least square error between model and observations. We also investigated a model that treats the mixed layer and pycnocline as being decoupled during the retreat phase (model II*b*), i.e.,

$$\Delta S = \frac{Qs\,\Delta t}{\hat{h}} \tag{14}$$

and from salt balance below the mixed layer, we find for small ΔS,

$$\Delta d = \frac{d}{S_b - S}\,\Delta S - \Delta h \tag{15}$$

i.e., during the retreat phase, model II*b* is equivalent to model II*a* with $\alpha_1 = 1$ and $\alpha_2 = d/(S_b - S)$. The entrainment phase is the same in both models. Model II*b* resulted in a better description of the annual cycle of d, but at the same time the model was poorer for S and h, so that the total error (scaled by the amplitude of the corresponding annual cycles) was larger for the model where the retreat was described by decoupled mixed layer and pycnocline (see section 5).

There are four parameters that determine the dynamics of the models II*a* and II*b*, two dissipation scales h_w and h_c, and α_1 and α_2, which correlate profile variations in the pycnocline with the entrainment rate and the rate of change of the mixed layer salinity. In order to determine whether the parameter α_2 was significant, we additionally tested the models I*a* and I*b*, which are equivalent to the models II*a* and II*b*, respectively, but with $\alpha_2 = 0$. For given fluxes at the surface and with given boundary conditions at $z = -h_b$, the evolution of the properties of the mixed layer and the seasonal pycnocline due to vertical mixing processes can now be described.

In addition to vertical mixing processes the profile parameters may be influenced by the oceanic flow field. Since the appropriate data set for comparing model and observed advective effects on the profile parameters during AIDJEX is not available, we will only briefly discuss how the advective scheme will be implemented into the coupled mixed layer–deep ocean model. Assuming that the velocity $\mathbf{u}(z)$ in the ocean is given from the momentum balance, the rate of change of the profile parameters due to advection is determined from the continuity equation and from the salt balance in both layers separately. There is no exchange of salt and heat between mixed layer and pycnocline in the advective scheme. The vertically integrated continuity equation yields an expression for the rate of change of the mixed layer depth

$$\frac{\partial h}{\partial t} = -\nabla \cdot (h\mathbf{u}) \tag{16}$$

where $\mathbf{u}$ is the velocity in the mixed layer. The conservation of salt in the mixed layer determines the rate of change of the mixed layer salinity.

$$\frac{\partial}{\partial t}(Sh) + \nabla \cdot (Sh\mathbf{u}) = 0 \tag{17}$$

Inserting (16) into (17) yields

$$\frac{\partial S}{\partial t} = -\mathbf{u} \cdot \nabla S \tag{18}$$

The conservation of salt in the pycnocline states that

$$\frac{\partial}{\partial t}\int_{-h_b}^{-h} S(z)\,dz + \nabla \cdot \int_{-h_b}^{-h} S(z)\mathbf{u}(z)\,dz = S_b w_b \tag{19}$$

where w_b is the vertical velocity at $z = -h_b$:

$$w_b = -\nabla \cdot \int_{-h_b}^{0} \mathbf{u}(z)\,dz \tag{20}$$

Vertical integration of the first term on the left-hand side of (19) together with (1) yields the rate of change of the pycnocline thickness:

$$\frac{\partial d}{\partial t} = \frac{1}{S_b - S}\left[\nabla \cdot \int_{-h_b}^{-h} S(z)\mathbf{u}(z)\,dz - S_b w_b + d\frac{\partial S}{\partial t} - S_b\frac{\partial h}{\partial t} + (h_b - h - d)\frac{\partial S_b}{\partial t}\right] \quad (21)$$

The advective change of S_b is determined through the coupling with the deep ocean part of the GCM.

The complete set of prognostic equations for the profile parameters is then given by the superposition of the advective effects (equations (16), (18), and (21)) and the changes due to the vertical mixing processes (equations (5), (6), and (10)).

4. Application to an Ice-Covered Ocean

The one-dimensional mixed layer model described in the previous section is now applied to an ice-covered ocean. In this case the seasonal variation of the air temperature (heating, cooling) has only a small effect on the temperature of the mixed layer. Observations during AIDJEX 1975–1976 indicate that the mixed layer temperature exhibits nearly no seasonal variation and is near the freezing point down to a depth of 60 m throughout the year [*McPhee*, 1978]. All net heat fluxes are used to freeze and melt ice. During ice melting, fresh water is added on top of the mixed layer that tends to stabilize the stratification. During the freezing period, brine is excluded from the newly formed ice, a layer of dense salty water destabilizes the stratification, and brine convection starts to develop.

Therefore the seasonal variation of surface air temperature manifests itself in a seasonally varying buoyancy flux, mainly due to positive freshwater flux in summer and negative freshwater flux (out of the mixed layer) during wintertime. Consequently, in contrast to the open ocean, the main variables of the dynamics of the polar mixed layer are salinity and depth.

There are two principle stirring mechanisms that may form a mixed layer: brine convection and mechanical mixing due to keel stirring introduced by the ice drift. Usually it is considered that brine convection is the most important mixing mechanism. One purpose of this paper is to show the relative importance of the mechanical mixing which has not conclusively been shown in previous studies [*Solomon*, 1973]. The two main driving forces of our polar mixed layer model are therefore the kinetic energy input due to mechanical stirring by the ice motion and the seasonally varying salt flux at the sea surface.

4.1. *Mechanical Mixing*

Since the ice is rather rough at the bottom, ice motion may be an effective mixing mechanism. The ice keels have an average depth of 5 m but may extend through the whole mixed layer (40–50 m). It was one of the major oceanographic goals during AIDJEX to express the drag between ice and ocean as a function of the speed of the ice relative to the undisturbed ocean. It was found that the drag could be expressed as

$$|\tau| = \rho C_w |\mathbf{V}|^2 \quad (22)$$

over a wide speed range, where $|\mathbf{V}|$ is the speed of the ice relative to the ocean below the frictional layer and the drag coefficient C_w was about 0.0034 [*McPhee*, 1975; *McPhee and Smith*, 1976]. The rate of working $\tilde{Q}_w$ (equation (7)) is then given by

$$\tilde{Q}_w = \mathbf{V} \cdot \boldsymbol{\tau} = \rho C_w |\mathbf{V}|^3 \cos\gamma \quad (23)$$

where γ is the frictional turning angle, found to be about 24°. Although a substantial amount of this energy is dissipated or carried away by internal waves (both effects are incorporated in the dissipation parameter D_w), ice keel stirring may be an effective mixing mechanism because typical friction velocities in the Arctic Ocean are of the order of 1 cm/s [*McPhee and Smith*, 1976]. The same order of magnitude is observed in the open ocean due to wind stress.

TABLE 1. Trend and Horizontal Gradients of the Mixed Layer Salinity S, Depth h, and e-Folding Depth d of the Pycnocline During AIDJEX

AIDJEX Camp	Trend			
	S, ‰/week	h, m/week	d, m/week	S_b, ‰/week
Caribou	0.013	−0.16	0.54	0.005
Blue Fox	0.014	−0.43	1.27	0.006
Snowbird	0.011	−0.29	0.37	0.002
	Horizontal Gradients			
	S, ‰/100 km	h, m/100 km	d, m/100 km	S_b, ‰/100 km
Caribou	0.21	−2.6	8.5	0.08
Blue Fox	0.13	−3.9	11.7	0.06
Snowbird	0.17	−4.6	5.8	0.04

4.2. *Surface Buoyancy Flux*

There were no ice thickness measurements undertaken during AIDJEX from which the surface buoyancy flux could have been estimated. Another way to determine the surface salt flux is to vertically integrate the salinity profiles. But it appears that the salinity is more variable at 60 m depth than at the surface, probably due to submerged eddies. Therefore the surface buoyancy flux can not be estimated from data, and we assume an analytical (asymmetric sinusoidal) form for the time dependence of the surface salt flux, which is determined by the melting and freezing rate F (Figure 6):

$$F(t) = a_m \sin(\pi t/t_m) \qquad 0 \le t \le t_m \quad (24a)$$

$$F(t) = a_f \sin[\pi(t + t_f - t_m)/t_f] \qquad t_m \le t \le t_m + t_f \quad (24b)$$

The amplitudes of melting (a_m) and freezing (a_f) in (24) can be determined by integrating F over the melting season t_m and freezing season t_f, respectively, which then has to equal the thickness A of the seasonally frozen or melted ice:

$$a_m = A\pi/2t_m \qquad a_f = A\pi/2t_f \quad (25)$$

The surface salinity source Q_s is now written as

$$Q_s = -F(S - S_I) \quad (26)$$

where S_I is the salinity of sea ice, taken to be 5‰. The surface salinity flux depends on two parameters, the annually frozen and melted ice thickness A and the length of the melting season t_m. Both surface flux parameters were determined in the

TABLE 2. Optimal Values of the Model Parameters α_1, α_2, h_w, h_c, the Surface Flux Parameters A, t_m, and the Root Mean Square Deviations Between Model and Data ε_s, ε_h, ε_d Obtained From a Least Squares Fit

AIDJEX Camp	Model	ε_s, ‰	ε_h, m	ε_d, m	α_1	α_2	h_w, m	h_c, m	A, m/yr	t_m, days
Caribou	I*a*	0.070	3.94	10.50	0.57	···	9.67	31.14	0.85	103
Caribou	I*b*	0.098	4.55	8.63	0.70	···	9.40	20.45	0.96	94
Caribou	II*a*	0.075	4.04	9.78	0.69	5.72	9.81	27.56	0.83	96
Caribou	II*b*	0.091	4.84	8.29	0.75	2.0	9.10	23.55	0.92	88
Blue Fox	I*a*	0.124	5.18	10.48	0.44	···	12.97	23.02	0.87	98
Blue Flox	I*b*	0.136	6.55	11.44	0.72	···	10.31	27.52	0.99	94
Snowbird	I*a*	0.076	4.48	13.44	0.57	···	10.29	21.41	1.37	99
Snowbird	I*b*	0.112	4.45	12.60	0.66	···	9.69	23.70	1.17	99

least squares sense from the observed data (Figure 5) together with the dynamical model parameters.

5. Comparison with AIDJEX Data

A complete comparison between observations and the model derived in the last section requires knowledge about the time histories (seasonal cycles) of the surface fluxes, salinity profiles, the ocean currents, and the horizontal gradients of the profile parameters at all locations where the model is to be tested. Unfortunately, these data are not available. Instead the available AIDJEX data provide information on salinity profiles measured from a drifting ice floe which traverses several hundred kilometers through different density regimes (Figure 2), thereby sampling the annual cycle of the salinity field at different times of the year at different locations. The observed annual increase in S, S_b, and d and decrease in h (Figure 5) is presumably largely due to the drift of the AIDJEX camps, since the ocean currents are generally slower than the ice drift.

There is no chance to rigorously derive advective effects from the AIDJEX data or other sources and compare them to the three-dimensional model predictions. But we believe that the one-dimensional model, describing the influence of surface fluxes and vertical mixing processes, which generally are responsible for most of the seasonal variations in the upper ocean, can be verified.

The problem arises of how to remove from the AIDJEX data information that is not due to vertical mixing processes. Since we have no data on surface buoyancy fluxes, we assume that the deviation of the surface fluxes from cyclostationarity is small and (24) can be used. The local equilibrium response of the ocean to cyclostationary surface fluxes is cyclostationary too. Therefore we have constructed a cyclostationary time series of the AIDJEX data by removing linear trends, such that the beginning and the end of the time series in Figure 5 match. The detrended data are shown as dots or crosses in Figure 7. The trend magnitudes for all parameters and stations are given in Table 1. Also given in Table 1 are estimates of the horizontal gradients of the profile parameters calculated as the ratio of the trend and the net distance that the camps travelled during AIDJEX. These horizontal gradients are generally in agreement with the known density field of the Beaufort Sea (Figure 2).

By removing linear trends, we assume that the effects of the drift of the AIDJEX camps and advection in the ocean are described by a linear function of time. Presumably, the actual drift effects are not quite linear in time. However, in view of the lack of data to determine the true time dependence and the fact that any guessed higher order function of time would unavoidably change the amplitude and the phase of the residual annual cycle, we think that for the time being our method is the appropriate way to create a cyclostationary time series which can be compared with the one-dimensional model predictions.

In order to fit our theoretical results to AIDJEX observations, we integrated the model outlined in sections 3 and 4 over 15 years, initialized with typical end of winter conditions using a fourth-order Runge-Kutta method and compared the last year (equilibrium annual cycle) to the detrended data of each AIDJEX camp separately. Then the model parameters α_1, α_2, h_w, h_c and the surface flux parameters A and t_m were changed, the model was then integrated again over 15 years, the final year again compared to data, and so on, until the least squares minimum was achieved. This least squares fit is preferred because it determines the optimal parameter values objectively instead of tuning them intuitively, as is usually done. All variables h, S, and d were fitted simultaneously, i.e., we minimized the error function E^2, given by

$$\min E^2 = \sum_{i=1}^{N} (h_i - \hat{h}_i)^2 W_h^2 + (S_i - \hat{S}_i)^2 W_s^2 + (d_i - \hat{d}_i)^2 W_d^2 \tag{27}$$

where N is the number of weekly data (50, 47, 46 for camps Caribou, Blue Fox, and Snowbird, respectively). $\hat{S}$, $\hat{h}$, and $\hat{d}$ denote the equilibrium annual cycle generated by the model, and S, h, and d represent the observations. The weighting functions W_s, W_h, and W_d were chosen to reflect the ratio of the amplitudes of the annual cycles of S, h, and d, so that $W_S : W_h : W_d = 90 : 2 : 1$.

S_b was fixed representing the observed detrended annual mean of the salinity at each camp at 150 m depth. The kinetic energy input (equation (23)) was taken as constant throughout the 15 years of integration, representing the corresponding observed annual mean of the camp drift velocity cubed. Including the observed weekly drift velocities would only be meaningful if the surface buoyancy flux were known as a weekly time series too, but this data was not available. For model I*a* fitted to camp Caribou data, we investigated the effect of the seasonal variation of the drift velocity on the model performance and parameter values. The camp drift velocity is approximately twice as big in summer as in winter but, presumably because of the with depth exponentially increasing energy loss (equation (11)), the effect of this difference on the model was only minor. The dissipation scales h_w and h_c changed by about 10%, the other parameters and the model errors even less.

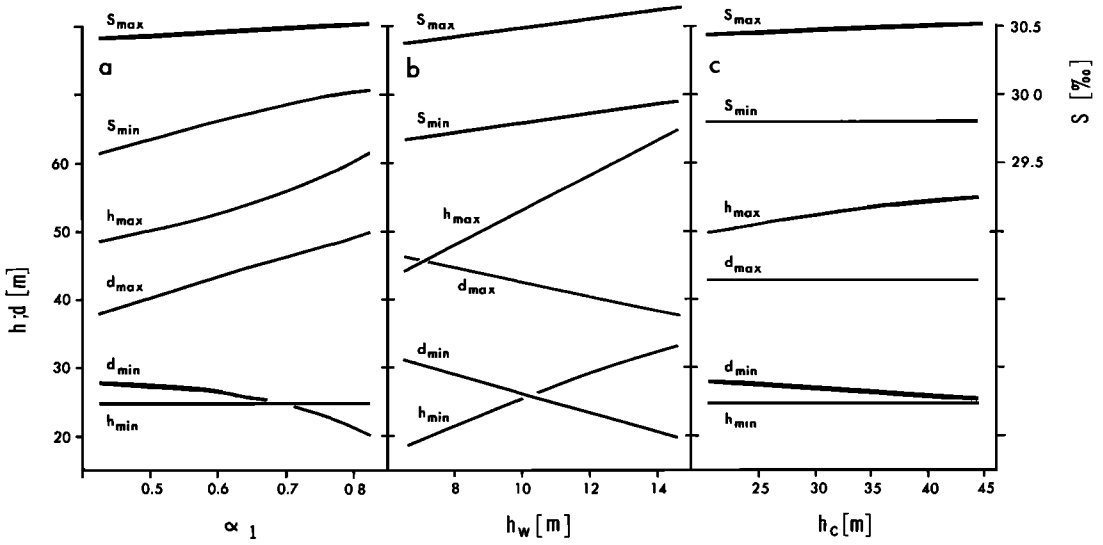

Fig. 8. Sensitivity of the equilibrium annual cycles of the model variables (model I*a*) with respect to the model parameters α_1, h_w, and h_c.

The optimal fit of the model equilibrium annual cycles for S, h, and d to the detrended Caribou data is shown in Figure 7. The model annual cycle was taken to begin with the onset of melting (retreat) which occurred during the 13th week of AIDJEX. The solid and dashed lines represent models I*a* and I*b*, respectively. The optimal values for the model parameters together with the root mean square deviations between model and data are shown in Table 2 for different models and camps.

Figure 7 and Table 2 show that except for Blue Fox the *b* models (decoupled layers during retreat) provide a better description of the pycnocline thickness d. However, at the same time the errors for the mixed layer salinity S and depth h are larger so that the total error (with the above mentioned weighting factors) is generally about 10% larger than for the *a* models. Models II*a* and II*b* did not provide a significant improvement. The total error was only about 1% smaller than for the models I*a* and I*b*, respectively. Therefore we conclude that the parameter α_2 is insignificant for modelling AIDJEX salinity data. Generally, the root mean square deviation between best fit model and data is about 10% to 15% of the observed amplitude of the annual cycles of the profile parameters.

The optimally fitted surface flux parameters A and t_m were about 0.9 m yr^{-1} for the annual surface fresh water source and sink and 95 days for the length of the melting season. These values are nearly independent of the model type and are also similar for all camps. Only Snowbird shows a slightly larger annual amplitude A for the fitted surface buoyancy flux and correspondingly also for the observed surface salinity. This could be explained with a larger amount of open water near the camp, leading to more melting and freezing. However, since the annual amplitude of the mixed layer depth was

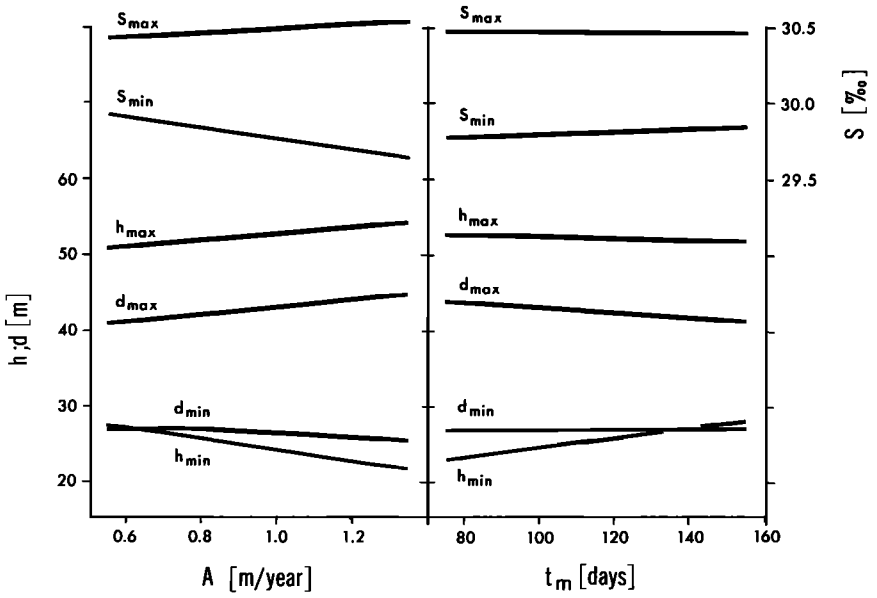

Fig. 9. Sensitivity of the equilibrium annual cycles of the model variables (model I*a*) with respect to the surface flux parameters A and t_m.

TABLE 3. Sensitivity of the Time of the Annual Minimum and Maximum of S, h, and d With Respect to Model and Surface Flux Parameters

	S_{max}	S_{min}	h_{max}	h_{min}	d_{max}	d_{min}
$\alpha = 0.4$	364	81	364	52	52	364
$\alpha = 0.6$	364	83	364	52	52	364
$\alpha = 0.8$	364	88	364	52	52	364
$h_w = 6.6$ m	364	84	364	52	52	364
$h_w = 9.6$ m	364	83	364	52	52	364
$h_w = 14.6$ m	364	83	2	52	52	2
$h_S = 19.0$ m	364	83	1	52	52	1
$h_S = 31.0$ m	364	83	364	52	52	364
$h_S = 46.0$ m	364	83	364	52	52	364
$A = 0.49$ m/yr	364	81	2	52	52	2
$A = 0.89$ m/yr	364	83	364	52	52	364
$A = 1.39$ m/yr	364	86	364	52	52	364
$t_m = 62$ days	364	50	364	32	32	364
$t_m = 102$ days	364	83	364	52	52	364
$t_m = 152$ days	364	125	2	77	77	2

nearly the same for all three camps, we think the larger annual cycle for the surface salinity is caused by the fact that Snowbird was likely to be the only camp that drifted in summer through the less dense center of the Beaufort gyre (see Figure 2), thereby amplifying the annual cycle of the mixed layer salinity. All other camps drifted more or less out of the gyre.

The optimally fitted scale depth of dissipation of surface mechanical energy input, $h_w \approx 10$ m, was also found to be nearly independent of model type and camp. With the annual mean of the mixed layer depth the dissipation parameter D_w (equation (11)) was estimated to be $D_w = 0.025$, which is approximately half of the corresponding value estimated by *Denman and Miyake* [1973] from records from ocean weather station Papa (50°N, 145°W; see also *Niiler and Kraus* [1977]).

The optimal scale depth of convective dissipation, $h_c \approx 25$ m, together with the annual mean of the mixed layer depth lead to a convective dissipation parameter $D_S = 0.22$ (equation (12)) which roughly agrees with the largest values obtained by *Farmer* [1975] for the observed mixed layer deepening under the ice of a frozen lake. The mean optimal value for the parameter α_1 which correlates the entrainment rate with changes of the pycnocline slope was found to be $\alpha_1 = 0.64$. Generally, the a models yielded a smaller value ($\alpha_1 = 0.57$) than the b models ($\alpha_1 = 0.71$).

In order to investigate the importance of the model parameters for the equilibrium solution, we performed several sensitivity tests with model Ia by changing the model parameters one at a time by $\pm 50\%$ about the optimal values and then integrating the model to equilibrium. The minimum and maximum values of the equilibrium annual cycle are shown in Figure 8 as a function of the model parameters α_1, h_w, and h_c and in Figure 9 as a function of the surface flux parameters A and t_m.

Figure 8 shows that the parameter α_1 affects the model variables in such a way that the amplitudes are increased for h and d and decreased for S. The dissipation scale depth h_w, on the other hand, keeps the amplitudes approximately constant. The convective dissipation scale depth h_c has only a minor influence of the equilibrium solution. Generally, a $\pm 50\%$ change in the model parameters leads to a response of the model variables which is less than $\pm 20\%$ for h and d and $\pm 2\%$ for S.

Figure 9 demonstrates that the model is less sensitive to changes in the surface flux parameters A and t_m than it is to α_1 and h_w. An increase in the amount of melting and freezing, A, leads to an increase in the amplitudes of all model variables, whereas a longer melting season t_m slightly decreases the amplitudes of S, h, and d.

In addition to the amplitudes, the time of the annual extrema is also influenced by the model and surface flux parameters. Table 3 shows that the winter extremum (S_{max}, h_{max}, d_{min}) is not affected at all. It is clear that the length of the melting season t_m has a noticeable effect on the summer extremum (S_{min}, h_{min}, d_{max}). Besides that, only the time of the minimum of the mixed layer salinity S is sensitive but even then only with respect to the parameters α_1 and A. Generally, the model exhibits only a moderate sensitivity to the fitted model and surface flux parameters.

Figure 10 shows the relative importance of the ice keel stirring and the surface buoyancy flux terms in the evolution of the mixed layer depth described by model Ia (equation (10)). During increased melting in the first half of summer, both terms are of the same size with opposite sign (definition of the retreat of the mixed layer, Monin-Obukhov length). From midsummer on the mixed layer deepens again because the buoyancy flux term rapidly decreases and becomes smaller in magnitude than the ice-keel stirring term. At the beginning of the freezing season the buoyancy flux term changes sign thereby contributing to the entrainment. In midwinter at the time of strongest freezing (by assumption of a sinusoidal time dependence; Figure 6) the convective deepening is approximately twice as big as the deepening due to the ice keel stirring.

6. CONCLUSIONS

The detrended data of the observed seasonal variations of the mixed layer salinity, the mixed layer depth, and the pycnocline thickness in the Beaufort Sea during AIDJEX can be successfully described by an extended one-dimensional Kraus-Turner type model that includes the pycnocline. In this model the dominant mixing mechanism that maintains the mixed layer in summer is the ice keel stirring. In wintertime the convective deepening due to brine expulsion from the newly formed ice is approximately twice as efficient as the mechanical mixing.

In addition to the surface stress and buoyancy flux the model depends on three parameters, two scale depths for the dissipation of mechanical and convective energy and a corre-

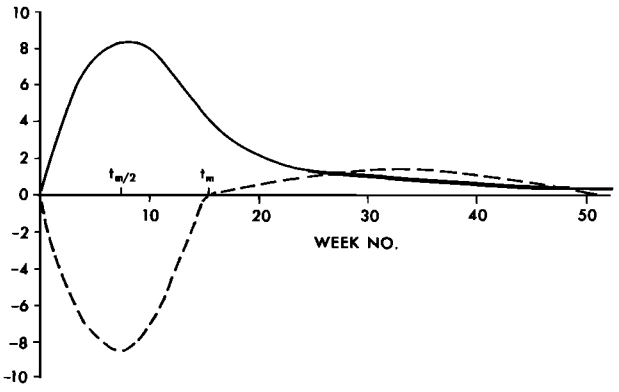

Fig. 10. Relative magnitudes of the ice keel stirring (solid line) and buoyancy flux (dashed line) terms in the evolution of the mixed layer depth (equation (10)).

lation coefficient between the entrainment rate and changes in the pycnocline thickness. The model is not very sensitive to moderate changes in these parameters about their optimal values.

The deviations between model and data are about 10% to 15% of the observed annual amplitudes. This error can probably be attributed mainly to short-term variations of the surface boundary conditions, the advection in the ocean, and the drift of the ice floe, which are not described in this paper.

Acknowledgments. The authors are grateful to K. Bryan, K. Hasselmann, K. Hunkins, and T. Yamagata for many stimulating discussions and comments on the original manuscript. This paper is an extension of a polar mixed layer model developed by the senior author during the Woods Hole Summer Study Program in Polar Oceanography in 1979 (Lemke, 1979). Discussion with the Summer School Staff, especially with P. Killworth and A. Gill, were very much appreciated. This work was partly supported by the Geophysical Fluid Dynamics Program, Princeton University/NOAA grant 04-7-022-44017, by the Max-Planck-Institut für Meteorologie, Hamburg, and by the Office of Naval Research contract N00014-76-C-0004 to Lamont-Doherty Geological Observatory of Columbia University. The oceanographic data were collected during the AIDJEX program with funding support by the Office of Naval Research. P. Lemke performed this work while on leave as a visiting scientist in the Geophysical Fluid Dynamics Program at Princeton University, Princeton, New Jersey. This is Lamont-Doherty Geological Observatory contribution number 3624.

REFERENCES

Adamec, D., R. L. Elsberry, R. W. Garwood, Jr., R. L. Haney, An embedded mixed layer-ocean circulation model, *Dyn. Atmos. Oceans, 6*, 69–96, 1981.

Bauer, E., K. Hunkins, T. O. Manley, and W. Tiemann, Arctic ice dynamics joint experiment 1975–1976 Physical oceanography data report, STD data, Camp Caribou, volume 1, *Tech. Rep. CU-8-80*, 529 pp., Lamont-Doherty Geol. Observ., Columbia Univ., Palisades, N. Y., 1980*a*.

Bauer, E., K. Hunkins, T. O. Manley, and W. Tiemann, Arctic ice dynamics joint experiment 1975–1976 Physical oceanography data report, STD data, Camp Blue Fox, volume 2, *Tech. Rep. CU-9-80*, 410 pp., Lamont-Doherty Geol. Observ., Columbia Univ., Palisades, N. Y., 1980*b*.

Bauer, E., K. Hunkins, T. O. Manley, and W. Tiemann, Arctic ice dynamics joint experiment 1975–1976 Physical oceanography data report, STD data, Camp Snowbird, volume 3, *Tech. Rep. CU-10-80*, 398 pp., Lamont-Doherty Geol. Observ., Columbia Univ., Palisades, N. Y., 1980*c*.

Bauer, E., K. Hunkins, T. O. Manley, and W. Tiemann, Arctic ice dynamics joint experiment 1975–1976 Physical oceanography data report, STD data, Camp Big Bear, volume 4, *Tech. Rep. CU-11-80*, 374 pp., Lamont-Doherty Geol. Observ., Columbia Univ., Palisades, N. Y., 1980*d*.

Denman, K. L., and M. Miyake, Upper layer modifications at ocean station Papa: Observations and simulation, *J. Physical Oceanogr., 3*, 185–196, 1973.

Farmer, D. M., Penetrative convection in the absence of mean shear, *Q. J. R. Meteorol. Soc., 101*, 869–891, 1975.

Hunkins, K. L., An estimate of the internal wave drag on pack ice, *AIDJEX Bull., 26*, 141–162, 1974.

Hunkins, K. L., The oceanic boundary layer and stress beneath a drifting ice flow, *J. Geophys. Res., 80*, 3425–3433, 1975.

Kim, J.-W., and W. L. Gates, Simulation of the seasonal fluctuation of the upper ocean by a global circulation model with an imbedded mixed layer, *Rep. 11*, 60 pages, Climatic Res. Inst., Oregon State Univ., Corvallis, 1980.

Lemke, P., A model for the seasonal variation of the mixed layer in the Arctic Ocean. Woods Hole Summer Study Program on Polar Oceanography, *Tech. Rep. WHOI-79-84*, pp. 82–96, Woods Hole Oceanogr. Inst., Woods Hole, Mass., 1979.

Maier-Reimer, E., D. Muller, D. Olbers, J. Willebrand, and K. Hasselmann, An ocean circulation model for climate variability studies, *Rep. 104 02 612*, Max-Planck Inst. für Meteorologie, Hamburg, Federal Republic of Germany, 1982.

Manley, T. O., Eddies of the western Arctic Ocean: Their characteristics and importance to the energy, heat and salt balance, *Tech. Rep. CU-1-80*, 426 pp., Lamont-Doherty Geol. Observ., Columbia Univ., Palisades, N. Y., 1981.

McPhee, M. G., The effect of ice motion on the mixed layer under Arctic pack ice. *AIDJEX Bull., 30*, 1–27, 1975.

McPhee, M. G., AIDJEX oceanographic data report, *AIDJEX Bull., 39*, 33–77, 1978.

McPhee, M. G., and J. D. Smith, Measurements of the turbulent boundary layer under pack ice, *J. Phys. Oceanogr., 6*, 696–711, 1976.

Morison, J., and J. D. Smith, Seasonal variations in the upper Arctic Ocean as observed at T-3, *Geophys. Res. Lett., 8*, 753–756, 1981.

Muench, R. D., P. H. LeBlond, and L. E. Hachmeister, On some possible interactions between internal waves and sea ice in the marginal ice zone, *J. Geophys. Res., 88*, 2819–2826, 1983.

Newton, J., The Canada Basin: Mean circulation and intermediate-scale flow features, doctoral dissertation, Univ. of Wash., Seattle, 1973.

Niiler, P. P., One-dimensional models of the seasonal thermocline, in *The Sea*, Vol. 6, edited by E. D. Goldberg, I. N. McCave, J. J. O'Brien, and J. H. Steele, pp. 97–115, John Wiley, New York, 1977.

Niiler, P. P., and E. B. Kraus, One-dimensional models of the upper ocean, in *Modelling and Prediction of the Upper Layers of the Ocean*, edited by E. B. Kraus, pp. 143–172, Pergamon, New York, 1977.

Pollard, D., M. L. Batteen, and Y.-J. Han, Development of a simple upper-ocean and sea ice model, *J. Phys. Oceanogr., 13*, 754–768, 1983.

Pritchard, R. S., (ed.) *Sea Ice Processes and Models*, University of Washington Press, Seattle, Wash., 1980.

Solomon, H., Wintertime surface layer convection in the Arctic Ocean, *Deep Sea Res., 20*, 269–283, 1973.

Thorndike, A. S., and T. O. Manley, Updated satellite positions for the AIDJEX manned camps, April 11, 1975 to October 17, 1975, *Tech. Rep. CU-9-80*, 347 pp., Lamont-Doherty Geol. Observ., Columbia Univ., Palisades, N. Y., 1980*a*.

Thorndike, A. S., and T. O. Manley, Updated satellite positions for the AIDJEX manned camps, October 19, 1975 to May 4, 1975, *Tech. Rep. CU-3-80*, 377 pp., Lamont-Doherty Geol. Observ., Columbia Univ., Palisades, N. Y., 1980*b*.

P. Lemke, Max-Planck-Institut für Meteorologie, Bundestrasse 55, 2000 Hamburg 13, Federal Republic of Germany.

T. O. Manley, Lamont-Doherty Geological Observatory of Columbia University, Palisades, NY 10964.

(Received June 17, 1983;
revised January 16, 1984;
accepted February 17, 1984.)